

Revisiting the Adversarial Robustness of Vision Language Models: a Multimodal Perspective

Wanqi Zhou^{1,2*}, Shuanghao Bai^{1*}, Qibin Zhao², Badong Chen^{1†}
¹Institute of Artificial Intelligence and Robotics, Xi'an Jiaotong University, China
²RIKEN AIP, Japan
 zwq785915792@stu.xjtu.edu.cn, baishuanghao@stu.xjtu.edu.cn
 qibin.zhao@riken.jp, chenbd@mail.xjtu.edu.cn

ABSTRACT

Pretrained vision-language models (VLMs) like CLIP have shown impressive generalization performance across various downstream tasks, yet they remain vulnerable to adversarial attacks. While prior research has primarily concentrated on improving the adversarial robustness of image encoders to guard against attacks on images, the exploration of text-based and multimodal attacks has largely been overlooked. In this work, we initiate the first known and comprehensive effort to study adapting vision-language models for adversarial robustness under the multimodal attack. Firstly, we introduce a multimodal attack strategy and investigate the impact of different attacks. We then propose a multimodal contrastive adversarial training loss, aligning the clean and adversarial text embeddings with the adversarial and clean visual features, to enhance the adversarial robustness of both image and text encoders of CLIP. Extensive experiments on 15 datasets across two tasks demonstrate that our method significantly improves the adversarial robustness of CLIP. Interestingly, we find that the model fine-tuned against multimodal adversarial attacks exhibits greater robustness than its counterpart fine-tuned solely against image-based attacks, even in the context of image attacks, which may open up new possibilities for enhancing the security of VLMs.

CCS CONCEPTS

• Computing methodologies → Artificial intelligence.

KEYWORDS

Adversarial training, vision language model, multimodal attack

1 INTRODUCTION

Pretrained vision-language models (VLMs) have demonstrated remarkable generalization capabilities across a wide range of downstream tasks, which become pivotal tools in the burgeoning field of multimodal artificial intelligence applications, such as image classification [17, 33], semantic segmentation [26] and robotics [45]. As a growing number of vision-language models are utilized in security-sensitive downstream tasks, enhancing the robustness of such models has become an urgent priority.

The CLIP model [33] boasts one of the most iconic frameworks and serves as the backbone for many other VLMs, making the study of its robustness particularly meaningful. Previous research on its robustness has primarily focused on image attacks from the visual domain [29, 40, 43], which reflects the initial perception that visual

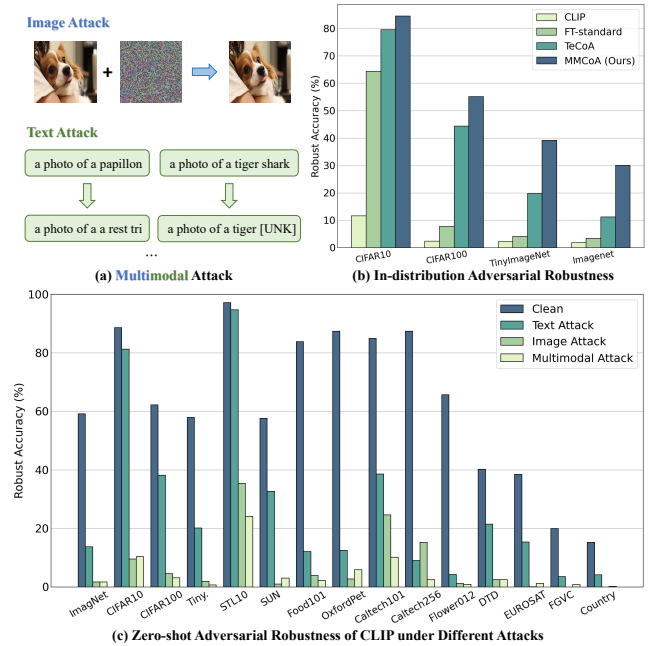


Figure 1: (a) An example of the multimodal adversarial attack. (b) The robust accuracies of different methods for in-distribution adversarial robustness under the multimodal attack. (c) The accuracies of CLIP for zero-shot adversarial robustness under different attacks.

data might be more susceptible or rewarding to adversarial manipulations. However, as the deployment of CLIP and other VLMs expands into increasingly diverse and complex environments, the necessity to scrutinize and fortify against a broader spectrum of vulnerabilities, including those in the language domain, becomes critical. In this study, we introduce an image-based PGD attack [27] and a text-based BERT-Attack [25]. As shown in Figure 1 (a), we combine these two attacks to formulate a multimodal attack strategy. As shown in Figure 1 (c), we observe that (1) imperceptible perturbations within the image domain significantly reduce the CLIP model's performance. (2) Under BERT-Attack, the more categories a dataset contains, the stronger the attack's efficacy. For instance, the accuracy decrease in CIFAR10 is less pronounced compared to the more substantial decline observed in CIFAR100. Therefore, enhancing the adversarial robustness of the text encoders in VLMs is also a challenge of paramount importance.

*Both authors contributed equally to this research.

†Corresponding author.

To counter the problem posed by adversarial examples, numerous defense methods have been proposed. Adversarial training [4] is considered one of the most effective defense strategies. Adversarial training from scratch for large-scale VLMs is impractical, thus previous methods mainly adopt adversarial training into prompt tuning and fine-tuning to defend against image-based attacks [29, 43]. However, as shown in Figure 1 (b), these methods fall short when facing multimodal attacks. To comprehensively bolster the adversarial robustness of the CLIP model, we propose a simple yet effective **Multimodal Contrastive Adversarial (MMCoA)** training framework, encompassing two key components: the text-supervised image adversarial loss and the image-supervised text adversarial Loss. The objective is to align the clean and adversarial visual features with their corresponding adversarial and clean text embeddings, respectively. By employing the multimodal adversarial training approach, we significantly bolster the adversarial robustness of CLIP against attacks spanning both image and language domains.

In this paper, we conduct an in-depth investigation of three types of attacks on 15 datasets, offering a comprehensive study assessing their impact on adversarial robustness across two distinct tasks. The first task is exploring in-distribution adversarial robustness, which tests defensive performance within the same dataset. The second task is exploring out-of-distribution generalization adversarial robustness, also referred to as zero-shot adversarial robustness, which evaluates defensive performance on unknown tasks. As illustrated in Figure 1 (b), our method markedly enhances the multimodal adversarial robustness of the CLIP model. Through comprehensive experiments and analyses, numerous novel and intriguing insights have emerged. Notably, we find that the model fine-tuned to counter multimodal adversarial attacks demonstrates superior robustness compared to the model fine-tuned exclusively against image-based attacks, even when facing image attacks. These findings suggest promising new avenues for bolstering the security framework of VLMs. Our main contributions can be summarized as follows:

- To the best of our knowledge, we initiate the first known and comprehensive effort to study adapting VLMs for adversarial robustness under the multimodal attack.
- We propose a simple yet effective **Multimodal Contrastive Adversarial** training loss, which can effectively enhance the adversarial robustness of both image and text encoders.
- Extensive experiments on 15 datasets for two tasks demonstrate that our method can significantly enhance the adversarial robustness of CLIP. Meanwhile, our detailed analyses can offer valuable insights to enhance the security of VLMs.

2 RELATED WORK

2.1 Adversarial Attack

The adversarial attack is first proposed in computer vision, creating perturbed images capable of deceiving deep learning models into incorrect classifications [38]. Then the gradient-based adversarial attacks have been extensively studied, including methods like FGSM [12], BIM and ILCM [23], and PGD [27]. The key idea of gradient-based methods is to find a minimal perturbation that maximizes the risk of making incorrect predictions, which can be easily achieved by applying gradient descent over the continuous space of images. In natural language processing, current successful attacks

for text usually adopt heuristic rules to modify the characters of a word [19, 25] or substitute words with synonyms [24, 34]. With the advent of VLMs, both modalities can be attacked simultaneously, thereby increasing the security vulnerabilities of such models. In this work, we integrate the image-based PGD attack [27] with the text-based attack [25] to formulate a multimodal attack. This marks the first endeavor to investigate the adaptation of the CLIP model for adversarial robustness under multimodal attack.

2.2 Adversarial Training

It has been discovered that deep neural networks are susceptible to adversarial attacks, and many defense approaches have been proposed, such as adversarial training [20, 30, 36], data transformation [2, 9, 15] and modifying the network [14, 35]. Adversarial training is considered one of the most effective strategies to improve the adversarial robustness of deep neural networks. This line of methods involves incorporating adversarial examples into the training process. Recent literature has extended adversarial training to vision-language models [29, 40, 43]. However, these studies have primarily concentrated on image-based attacks, incorporating adversarial examples derived from images into the fine-tuning of VLMs. Different from previous work, we explore the more complex challenge of multimodal defense. To bolster the robustness of both the image and text encoders in CLIP, we introduce a multimodal contrastive adversarial training framework. Our method aims to align clean and adversarial text embeddings with the adversarial and clean visual features, ensuring coherence between modalities even in the presence of adversarial perturbations.

2.3 Adapting Vision Language Models

Adapting the vision-language model CLIP for specific downstream tasks typically involves a fine-tuning approach. For instance, linear probing [33] focuses on training an additional classifier atop the image encoder of CLIP. Partial fine-tuning and full fine-tuning updates the last few layers of the model and the whole model, respectively. Recently, parameter-efficient fine-tuning methods have been extensively studied [18, 21, 44]. These methods only introduce a small set of parameters while keeping the large model fixed, including prompt tuning and adapter. Prompt tuning involves adding tunable parameters to the model's input, which are then optimized in a data-driven fashion via backpropagation, and it has been extensively studied in many downstream tasks [1, 5, 37]. On the other hand, adapters [11] typically consist of two fully connected layers with biases, separated by a non-linear activation function, seamlessly integrated into the base model. This design allows for targeted modifications without the need for extensive retraining of the entire model architecture. For the downstream task of adversarial learning, the adaptation of large-scale VLMs for multimodal and text adversarial robustness remains unexplored. In this study, we primarily utilize full fine-tuning as our methodological framework to showcase the potential of multimodal adversarial fine-tuning. Our findings suggest that our method could yield stronger robustness compared to unimodal adversarial fine-tuning, potentially opening up new possibilities for enhancing the security of VLMs.

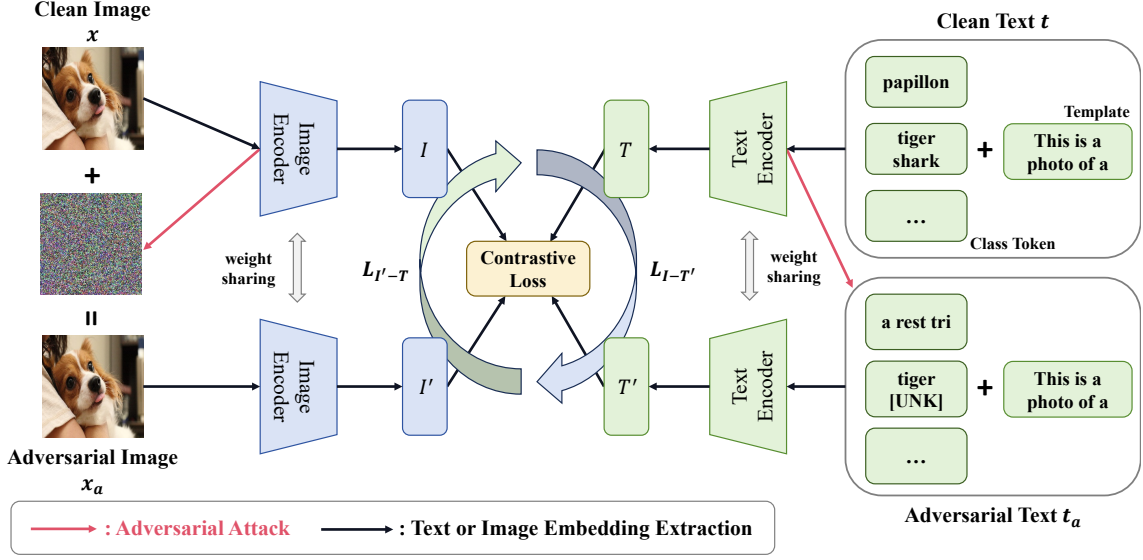


Figure 2: Overview of our proposed Multimodal Contrastive Adversarial (MMCoA) training framework. To achieve multimodal adversarial robustness, we extend the adversarial training paradigm to the joint training of adversarial examples for both images and texts by adversarial contrastive learning with vision and language supervision.

3 MULTIMODAL DEFEND FOR VISION LANGUAGE MODELS

3.1 Background and Problem Setup

Revisiting CLIP. We build our study of multimodal adversarial robustness on a pre-trained vision-language model CLIP [33]. Contrastive Language-Image Pre-Training (CLIP) model is pre-trained on 400 million image-text pairs collected from the internet with contrastive learning. It is composed of an image encoder f and a text encoder g , which are adopted to encode images x and their corresponding natural language descriptions t , respectively.

For adapting CLIP to downstream tasks, the natural language descriptions t are usually manually designed as "This is a photo of a [CLS].", where [CLS] denotes the class labels from a dataset. For zero-shot classification, the prediction \hat{y} of an image x is calculated:

$$p(\hat{y} | x) = \frac{\exp(\langle g(t_{\hat{y}}), f(x) \rangle / \tau)}{\sum_{j=1}^K \exp(\langle g(t_j), f(x) \rangle / \tau)}, \quad (1)$$

where $\langle \cdot, \cdot \rangle$ denotes the cosine similarity, τ denotes temperature parameter and K denotes the number of classes.

Multimodal Attack. In this study, the multimodal attack is combined with the image-based PGD attack [27] and text-based BERT-Attack [25]. The Projected Gradient Descent (PGD) attack is a popular adversarial attack method designed to create adversarial examples that deceive machine learning models. It iteratively applies gradient ascent techniques on the input data to maximize the cross-entropy loss \mathcal{L} , thereby generating an adversarial sample within a predefined perturbation limit that aims to maximize the error rate of the model. The core of the PGD algorithm unfolds through iterative steps, detailed below:

$$x_{k+1} = \Pi_{x+S} (x_k + \alpha \cdot \text{sign}(\nabla_x \mathcal{L}(\theta, x_k, y))), \quad (2)$$

where θ denotes the model parameters, y represents the ground-truth label, α is the step size, and Π_{x+S} refers to the projection onto the perturbation set defined by the ϵ -ball around x under the L_∞ or L_2 norm, ensuring the adversarial perturbation remains within the acceptable limits. The PGD attack method seeks to find an optimal yet human-imperceptible perturbation that misleads neural models with predefined bounds. As shown in Figure 2, the final adversarial image examples are denoted by x_a .

BERT-Attack is an adversarial attack method tailored for the BERT model or other models with transformer-based architectures. BERT-Attack targets text data, generating adversarial examples by modifying, inserting, or deleting words in the input text t . The core idea of BERT-Attack leverages a pre-trained language model to identify and replace the vulnerable words in the input text t that have the most significant impact on the model's prediction, thereby maximizing the model's output error. The adversarial text input is obtained by maximizing the divergence in the feature space between the perturbed text and the original text, employing measures such as KL divergence. BERT is utilized specifically to craft these adversarial examples, ensuring semantic consistency:

$$t_a = R(t), \quad (3)$$

$$\text{s.t. } t_a = \arg \max_{t_a} (\|g(t_a) - g(t)\|),$$

where $R(\cdot)$ denotes the operation of replacing or modifying tokens in the input text, and $g(\cdot)$ denotes the text encoder.

As shown in Figure 2, given that class tokens have a more pronounced impact on the model's prediction, replacements predominantly occur with these tokens.

Table 1: In-distribution robust accuracies across 4 datasets under three types of attacks, i.e., image attack, text attack and multimodal attack. Except for CLIP, we fine-tune all methods on each dataset and then test them on the same dataset. For image attacks, we utilize 100 steps of PGD, while text attacks are conducted using BERT-Attack. Δ denotes the difference in accuracy between our method and a baseline. Bold denotes the best accuracies.

| Method | CIFAR10 | | | CIFAR100 | | |
|------------------|--------------|--------------|-------------------|--------------|--------------|-------------------|
| | Image Attack | Text Attack | Multimodal Attack | Image Attack | Text Attack | Multimodal Attack |
| CLIP [33] | 9.32 | 79.74 | 11.65 | 4.59 | 37.24 | 2.42 |
| FT-standard [40] | 63.93 | 96.21 | 64.39 | 6.53 | 62.28 | 7.74 |
| TeCoA [29] | 85.06 | 92.04 | 79.53 | 60.71 | 56.96 | 44.34 |
| MMCoA (Ours) | 84.55 | 96.16 | 84.52 | 59.50 | 75.38 | 55.13 |
| Δ (CLIP) | +75.23 | +16.42 | +72.87 | +54.91 | +38.14 | +52.71 |
| Δ (SOTA) | -0.51 | -0.05 | +4.99 | -1.21 | +13.10 | +10.79 |
| Method | TinyImagenet | | | ImageNet | | |
| | Image Attack | Text Attack | Multimodal Attack | Image Attack | Text Attack | Multimodal Attack |
| CLIP [33] | 1.93 | 19.67 | 2.18 | 0.79 | 13.65 | 1.80 |
| FT-standard [40] | 4.55 | 29.96 | 4.10 | 3.88 | 17.61 | 3.47 |
| TeCoA [29] | 49.01 | 25.09 | 19.80 | 41.47 | 15.84 | 11.96 |
| MMCoA (Ours) | 53.97 | 54.13 | 39.19 | 46.58 | 41.34 | 30.02 |
| Δ (CLIP) | +52.04 | +34.46 | +37.01 | +45.79 | +27.69 | +28.22 |
| Δ (SOTA) | +4.96 | +24.17 | +19.39 | +5.11 | +25.50 | +18.06 |

Adversarial Training is a typical method for learning deep neural networks that are robust to adversarial attacks. Previous methods have mainly concentrated on defending against image-based attacks by fine-tuning models with adversarially generated image examples. Thus the training process can be formulated as:

$$\theta = \arg \min_{\theta} \mathcal{L}(\theta, x_a, y). \quad (4)$$

For large-scale vision-language models, it is essential not only to defend against image attacks but also to counteract textual attacks. Therefore, the adversarial training paradigm extends to the joint training of adversarial examples for both images and texts, which can be formulated as:

$$\theta = \arg \min_{\theta} \mathcal{L}(\theta, x_a, t_a, y). \quad (5)$$

3.2 Multimodal Contrastive Adversarial Training

To enhance the adversarial robustness of both image and text encoders, we propose a simple yet effective **Multimodal Contrastive Adversarial** (MMCoA) training method with contrastive losses, whose framework is illustrated in Figure 2. MMCoA consists of two contrastive losses, including *text-supervised image adversarial* contrastive loss and *image-supervised text adversarial* contrastive loss. We introduce our MMCoA in detail as follows.

Text-supervised Image Adversarial Training. Firstly, we generate a set of adversarial image examples with the image-based attack as depicted in section 3.1. As shown in Figure 1 (c), this misalignment can significantly degrade the model’s performance, as it struggles to associate the manipulated visual information with the

correct textual context. Text-supervised image adversarial training aims to minimize the feature distance between the attacked image x_a and the correct corresponding text inputs t .

For each image, we utilize the images and the corresponding manually crafted prompts, "This is a photo of a [CLS].", to form image-text pairs. Subsequently, we apply the text-supervised image adversarial contrastive loss, which can be formulated as:

$$\mathcal{L}_{I'-T}(x_a, t, \mathbf{y}) = -\mathbb{E}_{i,j} \left[y_{ij} \log \frac{\exp(\langle I'_i, T_j \rangle / \tau)}{\sum_k \exp(\langle I'_i, T_k \rangle / \tau)} \right], \quad (6)$$

$$\text{s.t. } y_{ij} = \begin{cases} 1, & i = j \\ 0, & i \neq j \end{cases},$$

where $I' = f(x_a)$ denotes the features of the adversarial input images, $T = g(t)$ denotes clean text embeddings, and \mathbf{y} denotes the contrastive labels for the image-text pairs.

Image-supervised Text Adversarial Training. Similar to text-supervised image adversarial training, we firstly transform the manually crafted prompt into adversarial text examples. To defend the text-based attack, the image-supervised text adversarial training is introduced to align the features between the clean image x and the adversarial corresponding text inputs t_a . Then, we apply the image-supervised text adversarial contrastive loss as follows:

$$\mathcal{L}_{I-T'}(x, t_a, \mathbf{y}) = -\mathbb{E}_{i,j} \left[y_{ij} \log \frac{\exp(\langle I_i, T'_j \rangle / \tau)}{\sum_k \exp(\langle I_i, T'_k \rangle / \tau)} \right], \quad (7)$$

$$\text{s.t. } y_{ij} = \begin{cases} 1, & i = j \\ 0, & i \neq j \end{cases},$$

Table 2: Out-of-distribution robust accuracies across 15 datasets under multimodal attack. Except for CLIP, we fine-tune all methods on ImageNet dataset with the few-shot setting (1-shot, 5-shot, and 50-shot) and full-shot setting, and then test them on the remaining datasets. For image attacks, we utilize 100 steps of PGD, while text attacks are conducted using BERT-Attack. Bold denotes the best accuracies.

| Method | Source | | | | | | | Target | | | | | | | | |
|------------------|--------------|--------------|--------------|--------------|--------------|--------------|-------------|--------------|-------------|--------------|--------------|-------------|-------------|--------------|-------------|--------------|
| | ImageNet | CIFAR10 | CIFAR100 | Tiny. | STL10 | SUN397 | Food101 | OxfordPets | Flower102 | DTD | EuroSAT | FGVCA. | Country211 | Caltech101 | Caltech256 | Average |
| CLIP [33] | 1.75 | 10.36 | 3.13 | 0.69 | 24.08 | 3.07 | 2.21 | 5.89 | 0.92 | 2.55 | 1.20 | 0.84 | 0.21 | 10.16 | 2.55 | 4.64 |
| <i>1-shot</i> | | | | | | | | | | | | | | | | |
| FT-standard [40] | 1.19 | 8.93 | 4.82 | 0.50 | 24.34 | 3.43 | 2.70 | 4.69 | 1.18 | 2.18 | 0.90 | 1.11 | 0.27 | 11.93 | 2.62 | 4.72 |
| TeCoA [29] | 1.77 | 10.05 | 3.18 | 0.73 | 23.84 | 3.06 | 2.18 | 5.78 | 0.99 | 2.34 | 1.02 | 0.84 | 0.26 | 10.26 | 2.56 | 4.59 |
| MMCoA (Ours) | 1.83 | 10.33 | 3.22 | 0.64 | 25.24 | 3.45 | 2.19 | 6.00 | 1.38 | 3.14 | 0.81 | 0.84 | 0.27 | 11.12 | 2.62 | 4.87 |
| <i>5-shot</i> | | | | | | | | | | | | | | | | |
| FT-standard [40] | 1.58 | 9.13 | 4.67 | 0.41 | 26.72 | 2.66 | 2.00 | 5.97 | 0.93 | 2.93 | 0.45 | 0.69 | 0.18 | 11.63 | 2.72 | 4.84 |
| TeCoA [29] | 2.55 | 17.69 | 4.42 | 0.39 | 38.39 | 4.52 | 1.45 | 4.14 | 1.63 | 2.93 | 0.80 | 0.96 | 0.36 | 13.94 | 2.24 | 6.43 |
| MMCoA (Ours) | 4.47 | 24.44 | 11.44 | 1.08 | 48.18 | 8.89 | 2.34 | 5.21 | 2.98 | 6.76 | 4.66 | 1.56 | 0.66 | 20.81 | 4.06 | 9.84 |
| <i>50-shot</i> | | | | | | | | | | | | | | | | |
| FT-standard [40] | 3.12 | 16.65 | 7.99 | 0.45 | 39.09 | 4.81 | 1.85 | 6.00 | 1.07 | 4.14 | 0.25 | 0.84 | 0.35 | 13.50 | 3.23 | 6.89 |
| TeCoA [29] | 7.17 | 40.97 | 16.28 | 5.29 | 68.94 | 17.64 | 4.15 | 6.49 | 3.45 | 11.86 | 1.87 | 2.07 | 1.12 | 31.80 | 5.93 | 15.00 |
| MMCoA (Ours) | 10.47 | 57.44 | 22.41 | 11.46 | 76.74 | 18.70 | 4.93 | 4.09 | 3.58 | 16.33 | 4.91 | 2.46 | 1.41 | 35.63 | 6.34 | 18.46 |
| <i>Full-shot</i> | | | | | | | | | | | | | | | | |
| FT-standard [40] | 3.47 | 16.77 | 8.11 | 1.24 | 41.16 | 4.95 | 1.60 | 5.61 | 1.45 | 3.24 | 0.32 | 1.47 | 0.36 | 15.73 | 2.95 | 7.23 |
| TeCoA [29] | 11.96 | 54.40 | 25.54 | 12.43 | 78.18 | 21.62 | 7.12 | 12.40 | 2.57 | 15.05 | 10.56 | 2.55 | 1.43 | 36.49 | 7.15 | 19.96 |
| MMCoA (Ours) | 22.89 | 61.47 | 29.31 | 17.66 | 82.99 | 21.94 | 4.53 | 15.59 | 2.49 | 7.71 | 14.07 | 1.86 | 1.53 | 38.69 | 7.23 | 22.00 |

where $I = f(x)$ denotes the features of the clean input images, $T' = g(t_a)$ denotes adversarial text embeddings. As a result, our MMCoA method can be trained end-to-end with a total contrastive loss, which can be formulated as:

$$\mathcal{L} = \gamma_1 \mathcal{L}_{I-T} + \gamma_2 \mathcal{L}_{I-T'}, \quad (8)$$

where γ_1 and γ_2 are hyper-parameters. Our method iteratively alternates between generating adversarial examples and updating the model via Equation 5. The adversarial robustness of both the image encoder and the text encoder is significantly enhanced through the strategic alignment of clean text embeddings with the image features of adversarial images and the alignment of adversarial text embeddings with the image features of clean images. This dual alignment fosters a robust multimodal representation, strengthening the model's defenses against various adversarial attacks.

4 EXPERIMENTS

4.1 Experimental Setup

Datasets. To explore in-distribution adversarial robustness, we choose 4 datasets, namely CIFAR10 [22], CIFAR100 [22], TinyImageNet [8], and ImageNet [8]. For the exploration of out-of-distribution generalization in adversarial robustness, we choose 15 datasets. Specifically, we fine-tune the models on ImageNet [8] and evaluate their performance on the remaining 14 datasets. These datasets are bifurcated into two principal categories: generic object

classification, which includes CIFAR10 [22], CIFAR100 [22], TinyImageNet (Tiny.) [8], STL10 [7], Caltech101 [10], and Caltech256 [13]; and fine-grained classification, featuring OxfordPets [32], Flowers102 [31], FGVC Aircraft (FGVCA.) [28], Food101 [3], EuroSAT [16], DTD [6], SUN397 [42], and Country211 [33]. Dataset details can be seen in the Appendix.

Baselines. Considering the limited research on the adversarial robustness of the CLIP model, we mainly include three baselines. One baseline is zero-shot CLIP [33] with the prompt "This is a photo of a [CLS]". FT-standard [40] refers to fine-tuning the model on clean datasets. TeCoA [29] refers to text-guided contrastive adversarial training, which uses additional information from the text embeddings to correct the visual features corrupted by the adversarial attacks. Details of baselines can be seen in the Appendix. **Implementation Details.** We mainly adopt the CLIP-B/32 architecture of the image encoder as our backbone. In our experiments, the hyperparameters γ_1 and γ_2 are set to 0.5, as specified in Equation 8. We employ the Adam optimizer for model optimization, with beta coefficients of 0.9 and 0.98, a weight decay parameter of 0.2, and an initial learning rate of $1e - 6$. Without additional specifications, for the adversarial training phase, we generate adversarial examples using a 10-step PGD routine, with a step size α of $1/255$ and a perturbation limit set to an L_∞ bound ϵ of $1/255$. For the testing phase, we generate adversarial examples for images via a

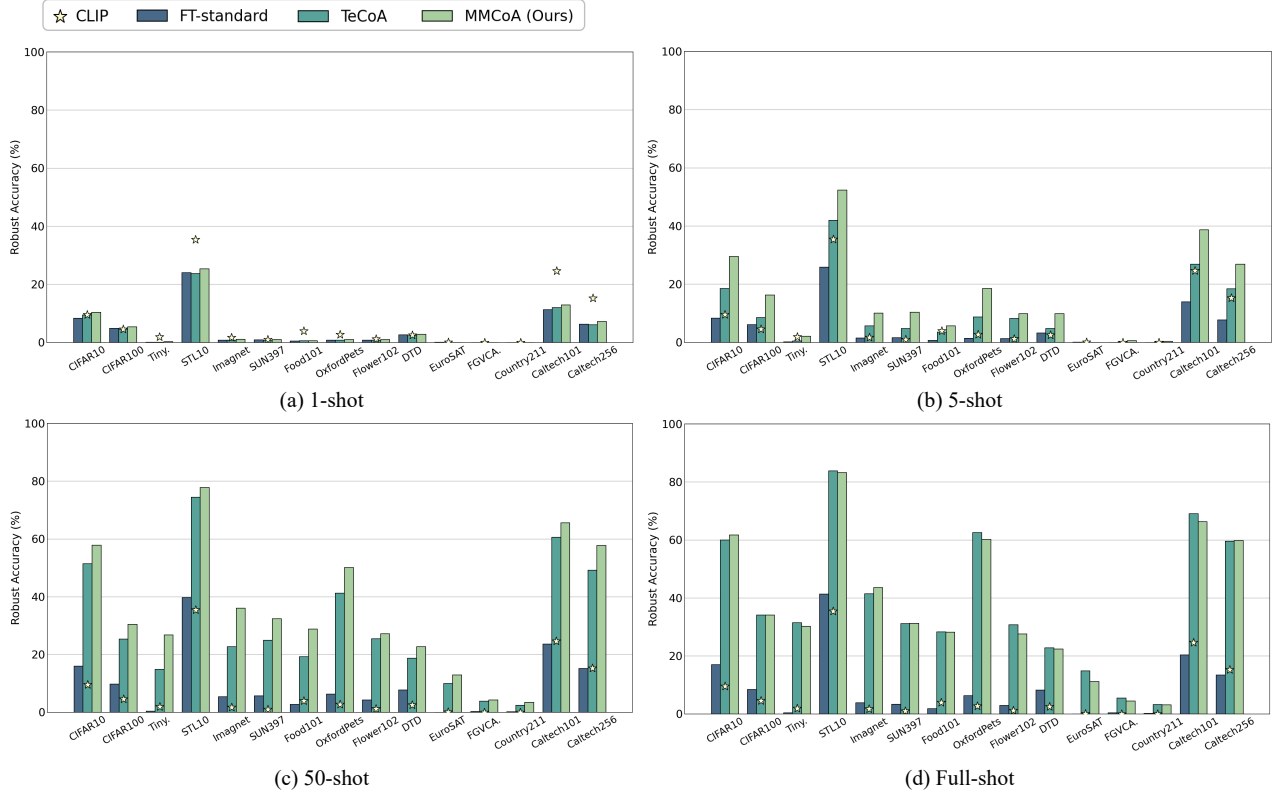


Figure 3: Out-of-distribution robust accuracies across 15 datasets under 100 steps of PGD image attack. We fine-tune all methods on ImageNet dataset with the few-shot setting and full-shot setting, and then test them on the remaining datasets.

100-step PGD method, each step exploring a step size α of $1/255$ with the perturbations bounded within an L_∞ ϵ ball of $1/255$.

4.2 Comparisons with Baselines

4.2.1 In-distribution Adversarial Robustness. For the in-distribution adversarial task, we aim to examine the impact of various attacks on the CLIP model and the effectiveness of adversarial learning algorithms in defending CLIP, particularly in scenarios where there is minimal distribution shift. To achieve this, we fine-tune the model using the training set of each dataset and then evaluate its performance on the test set of the same dataset.

As shown in Table 1, we evaluate the in-distribution adversarial robustness across four datasets under three types of attacks. When occurring with a small distribution shift, we have the following main findings as follows:

(1) Multimodal adversarial training significantly enhances the adversarial robustness of both the image and text encoders. Compared with CLIP, MMCoA can outperform CLIP on four datasets with a large margin of around 45%~75%, 16%~38%, 28%~72% under image attack, text attack, and multimodal attack, respectively. Additionally, under multimodal attack, our MMCoA method significantly surpasses all baseline methods, demonstrating a substantial margin of improvement.

(2) The strength between image attack and text attack. Combining the results from Figure 1 and Table 1, we observe that 1) *image attack has the potential to be more potent than text attack.* Specifically, 100-step PGD image attack significantly compromises the adversarial robustness of CLIP. For instance, for CIFAR10, the accuracy declines from 88.57% to 9.32% under image attack, but under text attack, it only drops to 79.74%. Similarly, for CIFAR100, the accuracy decreases from 62.22% to 4.59% under image attack, whereas under text attack, it reduces to 37.24%. 2) *As the number of categories in a dataset increases, text attacks become progressively stronger.* By comparing the results of CIFAR10 (10 classes), CIFAR100 (100 classes), TinyImageNet (200 classes), and ImageNet (1000 classes), we observe a trend of decreasing accuracy, with the extent of the decline growing more significant.

(3) As the number of categories in a dataset increases, multimodal adversarial training is more effective than image adversarial training. Compared with TeCoA, a specialized adversarial fine-tuning algorithm designed to counter image attacks, our MMCoA may perform slightly worse on datasets with fewer categories, such as CIFAR10 and CIFAR100. However, as the number of categories in the experimental datasets increases, our MMCoA can even surpass TeCoA in defending image attack.

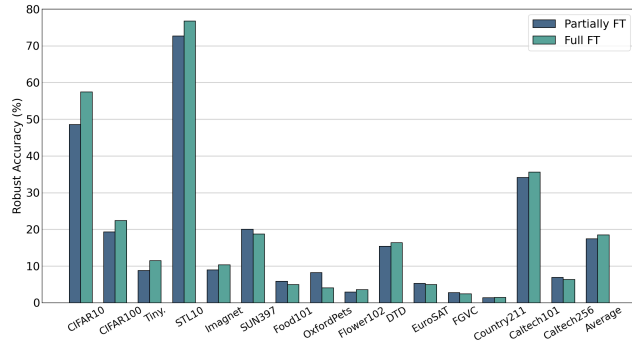


Figure 4: Exploration of the effect of the number of fine-tuned parameters with out-of-distribution generalization adversarial task on 15 datasets.

Table 3: Ablation on each constraint loss across 4 datasets with the in-distribution adversarial task. Average accuracies under three types of attacks are reported, i.e., image attack (I. A.), text attack (T. A.), and multimodal attack (M.M. A.).

| Exp. | \mathcal{L}_{I-T} | $\mathcal{L}_{I-T'}$ | Clean | I. A. | T. A. | M.M. A. |
|-------|---------------------|----------------------|--------------|--------------|-------|--------------|
| (a) | | | 67.37 | 4.16 | 37.58 | 4.51 |
| (b) | ✓ | | 66.78 | 44.68 | 41.12 | 30.64 |
| (c) | | ✓ | 76.07 | 10.70 | 73.42 | 12.21 |
| MMCoA | ✓ | ✓ | 80.40 | 61.15 | 66.75 | 52.22 |

(4) **Fine-tuning is a useful strategy for adapting VLMs to defend adversarial attacks.** It’s noteworthy that even when fine-tuning the CLIP model with a clean dataset or solely through image adversarial learning, its adversarial robustness is enhanced across three types of attacks. This indicates that fine-tuning can adapt the model to a specific dataset, resulting in an overall improvement in the model’s adversarial robustness within that dataset.

4.2.2 *Out-of-distribution Generalization Adversarial Robustness.* For the out-of-distribution generalization adversarial task, our objective is to explore the effectiveness of adversarial training on the CLIP model, when there is a significant distribution difference between the training and testing sets. To this end, we fine-tune the model using ImageNet as the training dataset and then evaluate its performance across 14 distinct downstream datasets.

It is important to highlight that findings (1), (2), and (4) detailed in subsection 4.2.1 remain valid even in scenarios with significant distribution shifts. As demonstrated in Table 2 and Figure 3, our additional findings are as follows:

(1) **The larger the training set size, the stronger the model’s adversarial robustness against multimodal and image attacks becomes.** We note that the accuracies of FT-standard, TeCoA, and our MMCoA improves as the volume of training data increases, enhancing robust accuracy.

(2) **Analysis of the adversarial robustness of baseline methods under multimodal and image attacks.** For FT-standard, fine-tuning with a clean dataset can enhance adversarial robustness,

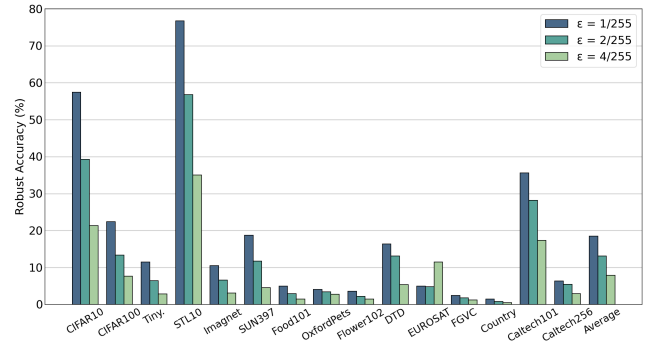


Figure 5: Exploration of the effect of the multimodal attack strength under different perturbation bounds with out-of-distribution generalization adversarial task on 15 datasets.

albeit marginally. In the case of TeCoA, its generalization capability is somewhat limited under a few-shot scenario. Nonetheless, with full-shot training, the improvement in adversarial robustness against multimodal and image attacks becomes significantly more pronounced. However, TeCoA still falls short of our MMCoA under multimodal attack. While TeCoA slightly outperforms our MMCoA under image attack, which is partly because MMCoA tends to overfit to the source dataset.

(3) **Our MMCoA is effective in few-shot scenarios under multimodal and image attacks,** where its generalization capability far surpasses that of the baselines. This demonstrates that our multimodal adversarial learning method can be significantly more efficient, making it an ideal choice for applications where data scarcity is a challenge. This balance between efficiency, effectiveness, and robust security underscores the potential of MMCoA as a leading solution in the field of adversarial machine learning.

4.3 Analysis

Effect of Each Constraint Loss. As shown in Table 3, when occurring with minimal distribution shifts, the omission of the two contrastive losses significantly decreases robust accuracy under all three types of attacks. With only the text-supervised image adversarial loss, there is a larger improvement in adversarial robustness against multimodal and image attacks. Conversely, when solely employing the image-supervised text adversarial loss, there is a notable enhancement in both clean accuracy and robust accuracy against text attack. Within our MMCoA framework, the two types of losses synergistically enhance performance, achieving state-of-the-art results in both clean accuracy and robust accuracy under multimodal and image attacks. However, compared with example (c), the introduction of image adversarial samples paradoxically tends to impair the adversarial robustness against text attack.

Effect of Number of Fine-tuned Parameters. In this case, we are testing the impact of solely fine-tuning the image encoder, which is referred to as partial fine-tuning. As shown in Figure 4, we demonstrate a comparison of robust accuracy between partially fine-tuning and full fine-tuning under multimodal attack. It is evident that the more parameters are trained, the stronger the model’s adversarial robustness becomes.

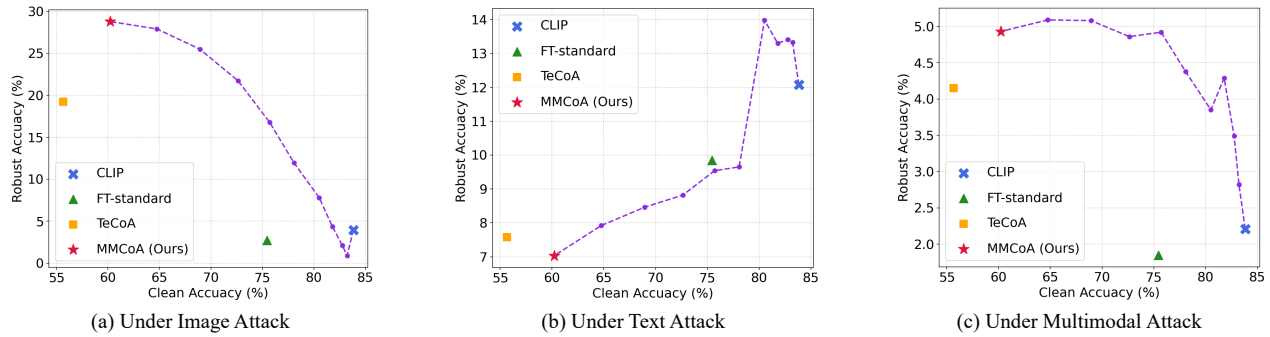


Figure 6: Relationship between the robust accuracy and the clean accuracy via weight interpolation. We test different methods on Food101 with 50-shot out-of-distribution generalization adversarial task under three types of attacks.

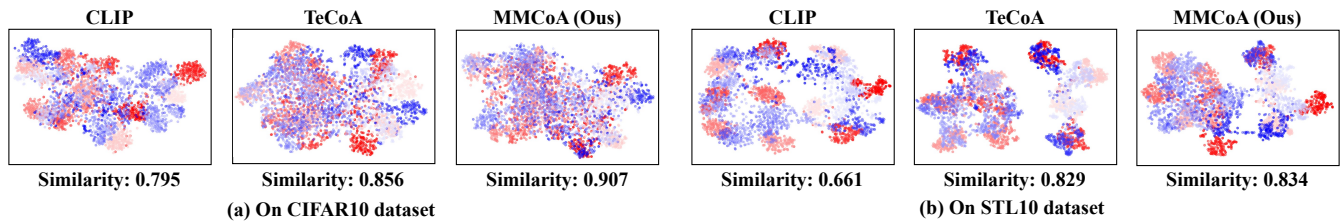


Figure 7: The t-SNE visualization on the CIFAR10 and STL10 datasets with CLIP, TeCoA, and our MMCoA for out-of-distribution generalization adversarial task. The clean and adversarial image features extracted from 10 classes are shown in blue and red, respectively. Different shades of color represent different classes.

Effect of Attack Strength. To investigate the impact of adversarial perturbation bounds on our method, we incrementally increased the perturbation bound for MMCoA among 1/255, 2/255, 4/255 of image attack under multimodal attack. As illustrated in Figure 5, our method exhibits a gradual decline in robust accuracy as the adversarial perturbation increases, with the decrease displaying a stepwise pattern.

Relationship between Robust and Clean Accuracy. As shown in Figure 6, under image and multimodal attacks, MMCoA exhibits a trade-off between robust accuracy and clean accuracy, striking the most optimal balance compared to other methods. However, we observe a simultaneous decline in robust and clean accuracies under text attack, suggesting that training with adversarial text samples may not be a prudent choice when faced with significant distribution shifts. Instead, training with clean text proves can be more effective against text attack. *For more analyses of the relationship between robust and clean accuracy, please refer to the appendix.*

T-SNE Visualizations. As shown in Figure 7, we visualize the clean and adversarial image features learned by CLIP, TeCoA, and MMCoA on two datasets. Qualitatively, we can observe that MMCoA achieves a higher degree of mix between clean and adversarial image features compared to baseline methods. Quantitatively, we calculate the cosine similarity between the clean and adversarial features for each image and computed the average value across all samples. We find that our MMCoA exhibits the highest similarity between clean and adversarial features for each image, demonstrating the effectiveness of MMCoA. *Due to the page limit, more*

detailed experiments and analyses can be found in the appendix. Furthermore, we comprehensively summarize the adversarial robustness characteristics of CLIP against three types of attacks and analyze its performance in terms of clean accuracy.

5 CONCLUSION

In this study, we initiate the first known and comprehensive effort to study adapting VLMs for adversarial robustness under three types of attacks. We explored the strength of three types of attacks across two tasks: in-distribution and out-of-distribution generalization adversarial tasks. Then we assessed the defensive capabilities of each method, the impact of the training set size on adversarial robustness, and the relationship between clean and robustness accuracy, among other aspects. To effectively enhance the adversarial robustness of both the image and text encoders within CLIP, we introduce a multimodal contrastive adversarial (MMCoA) training framework. Through extensive experiments, we demonstrate the effectiveness of our MMCoA framework, and our detailed analyses offer valuable insights for adapting large-scale VLMs to enhance their adversarial robustness against three types of attacks. We hope that our findings can pave the way for promising new strategies to strengthen the security frameworks of VLMs.

ACKNOWLEDGMENTS

This work was supported by the National Natural Science Foundation of China with grant numbers (U21A20485, 62088102, 61976175).

REFERENCES

- [1] Shuanghao Bai, Min Zhang, Wanqi Zhou, Siteng Huang, Zhirong Luan, Donglin Wang, and Badong Chen. 2024. Prompt-based distribution alignment for unsupervised domain adaptation. In *Proceedings of the AAAI Conference on Artificial Intelligence*, Vol. 38. 729–737.
- [2] Arjun Nitin Bhagoji, Daniel Cullina, Chawin Sitawarin, and Prateek Mittal. 2018. Enhancing robustness of machine learning systems via data transformations. In *2018 52nd Annual Conference on Information Sciences and Systems (CISS)*. IEEE, 1–5.
- [3] Lukas Bossard, Matthieu Guillaumin, and Luc Van Gool. 2014. Food-101—mining discriminative components with random forests. In *Computer Vision—ECCV 2014: 13th European Conference, Zurich, Switzerland, September 6–12, 2014, Proceedings, Part VI 13*. Springer, 446–461.
- [4] Tianlong Chen, Sijia Liu, Shiyu Chang, Yu Cheng, Lisa Amini, and Zhangyang Wang. 2020. Adversarial robustness: From self-supervised pre-training to fine-tuning. In *Proceedings of the IEEE/CVF conference on computer vision and pattern recognition*. 699–708.
- [5] Junhyeong Cho, Gilhyun Nam, Sungyeon Kim, Hunmin Yang, and Suha Kwak. 2023. Promptstyler: Prompt-driven style generation for source-free domain generalization. In *Proceedings of the IEEE/CVF International Conference on Computer Vision*. 15702–15712.
- [6] Mircea Cimpoi, Subhansu Maji, Iasonas Kokkinos, Sammy Mohamed, and Andrea Vedaldi. 2014. Describing textures in the wild. In *Proceedings of the IEEE conference on computer vision and pattern recognition*. 3606–3613.
- [7] Adam Coates, Andrew Ng, and Honglak Lee. 2011. An analysis of single-layer networks in unsupervised feature learning. In *Proceedings of the fourteenth international conference on artificial intelligence and statistics*. JMLR Workshop and Conference Proceedings, 215–223.
- [8] Jia Deng, Wei Dong, Richard Socher, Li-Jia Li, Kai Li, and Li Fei-Fei. 2009. Imagenet: A large-scale hierarchical image database. In *2009 IEEE conference on computer vision and pattern recognition*. Ieee, 248–255.
- [9] Gintare Karolina Dziugaite, Zoubin Ghahramani, and Daniel M Roy. 2016. A study of the effect of jpg compression on adversarial images. *arXiv preprint arXiv:1608.00853* (2016).
- [10] Li Fei-Fei, Rob Fergus, and Pietro Perona. 2004. Learning generative visual models from few training examples: An incremental bayesian approach tested on 101 object categories. In *2004 conference on computer vision and pattern recognition workshop*. IEEE, 178–178.
- [11] Peng Gao, Shijie Geng, Renrui Zhang, Teli Ma, Rongyao Fang, Yongfeng Zhang, Hongsheng Li, and Yu Qiao. 2024. Clip-adapter: Better vision-language models with feature adapters. *International Journal of Computer Vision* 132, 2 (2024), 581–595.
- [12] Ian J Goodfellow, Jonathon Shlens, and Christian Szegedy. 2014. Explaining and harnessing adversarial examples. *arXiv preprint arXiv:1412.6572* (2014).
- [13] Gregory Griffin, Alex Holub, and Pietro Perona. 2007. Caltech-256 object category dataset. (2007).
- [14] Shixiang Gu and Luca Rigazio. 2014. Towards deep neural network architectures robust to adversarial examples. *arXiv preprint arXiv:1412.5068* (2014).
- [15] Chuan Guo, Mayank Rana, Moustapha Cisse, and Laurens Van Der Maaten. 2017. Countering adversarial images using input transformations. *arXiv preprint arXiv:1711.00117* (2017).
- [16] Patrick Helber, Benjamin Bischke, Andreas Dengel, and Damian Borth. 2018. Introducing eurosat: A novel dataset and deep learning benchmark for land use and land cover classification. In *IGARSS 2018-2018 IEEE international geoscience and remote sensing symposium*. IEEE, 204–207.
- [17] Chao Jia, Yinfei Yang, Ye Xia, Yi-Ting Chen, Zarana Parekh, Hieu Pham, Quoc Le, Yun-Hsuan Sung, Zhen Li, and Tom Duerig. 2021. Scaling up visual and vision-language representation learning with noisy text supervision. In *International conference on machine learning*. PMLR, 4904–4916.
- [18] Menglin Jia, Luming Tang, Bor-Chun Chen, Claire Cardie, Serge Belongie, Bharath Hariharan, and Ser-Nam Lim. 2022. Visual prompt tuning. In *European Conference on Computer Vision*. Springer, 709–727.
- [19] Di Jin, Zhijing Jin, Joey Tianyi Zhou, and Peter Szolovits. 2019. Is bert really robust? natural language attack on text classification and entailment. *arXiv preprint arXiv:1907.11932* 2 (2019), 10.
- [20] Gaojie Jin, Xinpeng Yi, Dengyu Wu, Ronghui Mu, and Xiaowei Huang. 2023. Randomized adversarial training via Taylor expansion. In *Proceedings of the IEEE/CVF Conference on Computer Vision and Pattern Recognition*. 16447–16457.
- [21] Muhammad Uzair Khattak, Hanoona Rasheed, Muhammad Maaz, Salman Khan, and Fahad Shahbaz Khan. 2023. Maple: Multi-modal prompt learning. In *Proceedings of the IEEE/CVF Conference on Computer Vision and Pattern Recognition*. 19113–19122.
- [22] Alex Krizhevsky, Geoffrey Hinton, et al. 2009. Learning multiple layers of features from tiny images. (2009).
- [23] Alexey Kurakin, Ian J Goodfellow, and Samy Bengio. 2018. Adversarial examples in the physical world. In *Artificial intelligence safety and security*. Chapman and Hall/CRC, 99–112.
- [24] Jinfeng Li, Shouling Ji, Tianyu Du, Bo Li, and Ting Wang. 2018. Textbugger: Generating adversarial text against real-world applications. *arXiv preprint arXiv:1812.05271* (2018).
- [25] Linyang Li, Ruotian Ma, Qipeng Guo, Xiangyang Xue, and Xipeng Qiu. 2020. Bert-attack: Adversarial attack against bert using bert. *arXiv preprint arXiv:2004.09984* (2020).
- [26] Timo Lüddecke and Alexander Ecker. 2022. Image segmentation using text and image prompts. In *Proceedings of the IEEE/CVF conference on computer vision and pattern recognition*. 7086–7096.
- [27] Aleksander Madry, Aleksandar Makelov, Ludwig Schmidt, Dimitris Tsipras, and Adrian Vladu. 2017. Towards deep learning models resistant to adversarial attacks. *arXiv preprint arXiv:1706.06083* (2017).
- [28] Subhansu Maji, Esa Rahtu, Juho Kannala, Matthew Blaschko, and Andrea Vedaldi. 2013. Fine-grained visual classification of aircraft. *arXiv preprint arXiv:1306.5151* (2013).
- [29] Chengzhi Mao, Scott Geng, Junfeng Yang, Xin Wang, and Carl Vondrick. 2022. Understanding zero-shot adversarial robustness for large-scale models. *arXiv preprint arXiv:2212.07016* (2022).
- [30] Seyed-Mohsen Moosavi-Dezfooli, Alhussein Fawzi, and Pascal Frossard. 2016. Deepfool: a simple and accurate method to fool deep neural networks. In *Proceedings of the IEEE conference on computer vision and pattern recognition*. 2574–2582.
- [31] Maria-Elena Nilsback and Andrew Zisserman. 2008. Automated flower classification over a large number of classes. In *2008 Sixth Indian conference on computer vision, graphics & image processing*. IEEE, 722–729.
- [32] Omkar M Parkhi, Andrea Vedaldi, Andrew Zisserman, and CV Jawahar. 2012. Cats and dogs. In *2012 IEEE conference on computer vision and pattern recognition*. IEEE, 3498–3505.
- [33] Alec Radford, Jong Wook Kim, Chris Hallacy, Aditya Ramesh, Gabriel Goh, Sandhini Agarwal, Girish Sastry, Amanda Askell, Pamela Mishkin, Jack Clark, et al. 2021. Learning transferable visual models from natural language supervision. In *International conference on machine learning*. PMLR, 8748–8763.
- [34] Shuhuai Ren, Yihe Deng, Kun He, and Wanxiang Che. 2019. Generating natural language adversarial examples through probability weighted word saliency. In *Proceedings of the 57th annual meeting of the association for computational linguistics*. 1085–1097.
- [35] Andrew Ross and Finale Doshi-Velez. 2018. Improving the adversarial robustness and interpretability of deep neural networks by regularizing their input gradients. In *Proceedings of the AAAI conference on artificial intelligence*, Vol. 32.
- [36] Swami Sankaranarayanan, Arpit Jain, Rama Chellappa, and Ser Nam Lim. 2018. Regularizing deep networks using efficient layerwise adversarial training. In *Proceedings of the AAAI Conference on Artificial Intelligence*, Vol. 32.
- [37] Manli Shu, Weili Nie, De-An Huang, Zhiding Yu, Tom Goldstein, Anima Anandkumar, and Chaowei Xiao. 2022. Test-time prompt tuning for zero-shot generalization in vision-language models. *Advances in Neural Information Processing Systems* 35 (2022), 14274–14289.
- [38] Christian Szegedy, Wojciech Zaremba, Ilya Sutskever, Joan Bruna, Dumitru Erhan, Ian Goodfellow, and Rob Fergus. 2013. Intriguing properties of neural networks. *arXiv preprint arXiv:1312.6199* (2013).
- [39] Bart Thomee, David A Shamma, Gerald Friedland, Benjamin Elizalde, Karl Ni, Douglas Poland, Damian Borth, and Li-Jia Li. 2016. Yfcc100m: The new data in multimedia research. *Commun. ACM* 59, 2 (2016), 64–73.
- [40] Sibow Wang, Jie Zhang, Zheng Yuan, and Shiguang Shan. 2024. Pre-trained Model Guided Fine-Tuning for Zero-Shot Adversarial Robustness. *arXiv preprint arXiv:2401.04350* (2024).
- [41] Mitchell Wortsman, Gabriel Ilharco, Jong Wook Kim, Mike Li, Simon Kornblith, Rebecca Roelofs, Raphael Gontijo Lopes, Hannaneh Hajishirzi, Ali Farhadi, Hongseok Namkoong, et al. 2022. Robust fine-tuning of zero-shot models. In *Proceedings of the IEEE/CVF conference on computer vision and pattern recognition*. 7959–7971.
- [42] Jianxiong Xiao, James Hays, Krista A Ehinger, Aude Oliva, and Antonio Torralba. 2010. Sun database: Large-scale scene recognition from abbey to zoo. In *2010 IEEE computer society conference on computer vision and pattern recognition*. IEEE, 3485–3492.
- [43] Jiaming Zhang, Xingjun Ma, Xin Wang, Lingyu Qiu, Jiaqi Wang, Yu-Gang Jiang, and Jitao Sang. 2023. Adversarial Prompt Tuning for Vision-Language Models. *arXiv preprint arXiv:2311.11261* (2023).
- [44] Kaiyang Zhou, Jingkang Yang, Chen Change Loy, and Ziwei Liu. 2022. Learning to prompt for vision-language models. *International Journal of Computer Vision* 130, 9 (2022), 2337–2348.
- [45] Brianna Zitkovich, Tianhe Yu, Sichun Xu, Peng Xu, Ted Xiao, Fei Xia, Jialin Wu, Paul Wohlhart, Stefan Welker, Ayyaan Wahid, et al. 2023. Rt-2: Vision-language-action models transfer web knowledge to robotic control. In *Conference on Robot Learning*. PMLR, 2165–2183.

This appendix is organized as follows:

- Section A provides the detailed dataset information.
- Section B provides the additional training implementation details.
- Section C gives additional experiment results and analyses, including additional comparisons with out-of-distribution generalization adversarial task under text attack, clean accuracy with two tasks, details ablation experiments on each loss, and effect of the number of iterations.
- Section D offers a detailed analysis and comprehensive conclusions regarding the performance under three types of attacks across two tasks.

A DATASET DETAILS

The 15 datasets fall into two categories: generic object classification and fine-grained classification. We introduce as follows.

A.1 Generic Object Classification Dataset

CIFAR10 [22] originates from the Tiny Images dataset, featuring 60,000 color images with dimensions of 32×32 . Each image is uniquely classified into one of ten distinct classes.

CIFAR100 [22] also derived from the Tiny Images, includes 60,000 color images, each measuring 32×32 pixels. CIFAR100 is organized into 100 classes, which are further aggregated into 20 superclasses for a structured classification framework.

TinyImageNet [8] offers a compact version of the ImageNet [8], containing 100,000 images across 200 classes, with each class providing 500 training images, alongside 50 validation and 50 test images, all resized to 64×64 pixels.

STL10 [7] is a subset of ImageNet [8]. It includes 13,000 color images with a resolution of 96×96 , representing 10 object classes.

Caltech101 [10] contains images from 101 object categories and a background category that contains the images not from the 101 object categories. For each object category, there are about 40 to 800 images, while most classes have about 50 images. The resolution of the image is roughly about 300×200 pixels.

Caltech256 [13] an extension of Caltech101 [10], is an object recognition dataset with 30,607 images of varying sizes across 257 categories (256 object classes plus one clutter class), ensuring a minimum of 80 images per class.

ImageNet [8] contains 14,197,122 annotated images according to the WordNet hierarchy, which is a large-scale image database. This expansive collection spans roughly 22,000 categories, encompassing a diverse array of subjects including various animals, plants, geographical locations, and common everyday items.

A.2 Fine-grained Classification Dataset

OxfordPets [32] is comprised of a dataset featuring 37 categories of pets, each represented by approximately 200 images. These images exhibit a broad variety in scale, pose, and lighting conditions. Each image is meticulously annotated with breed information, a region of interest (ROI) for the head, and pixel-level trimap segmentation for detailed analysis.

Flower102 [31] introduces a dataset of 102 flower categories, selected for their common occurrence in the United Kingdom. Each category contains between 40 and 258 images. Detailed information

on the categories and the specific number of images per class is accessible through the category statistics page.

FGVCAircraft [28] encompasses 10,200 images across 102 different aircraft model variants, predominantly featuring airplanes. Each image highlights the main aircraft within a precise bounding box and is classified using a hierarchical airplane model label, organized across four levels of hierarchy.

Food101 [3] includes 101 food categories, each with 750 training images and 250 test images, totaling 101,000 images. The test images have undergone manual cleanup to ensure label accuracy, whereas the training set may include some level of noise.

EuroSAT [16] is a dataset and deep learning benchmark for land use and land cover classification. The dataset is based on Sentinel-2 satellite images covering 13 spectral bands and consisting of 10 classes with in total of 27,000 labeled and geo-referenced images.

DTD [6] offers 5,640 images of natural textures, annotated with attributes that reflect the perceptual properties of textures as perceived by humans. Organized by a list of 47 perceptually inspired terms, DTD includes 120 images for each category. Image sizes vary, and each predominantly showcases the texture attribute it represents. Sourced from Google and Flickr, these images were annotated via Amazon Mechanical Turk through multiple rounds. **SUN397** [42] contains 899 categories and 130,519 images. There are 397 well-sampled categories to evaluate numerous state-of-the-art algorithms for scene recognition.

Country211 [33] is a dataset released by OpenAI, designed to assess the geolocation capability of visual representations. It filters the YFCC100m [39] to find 211 countries that have at least 300 photos with GPS coordinates. OpenAI built a balanced dataset with 211 categories, by sampling 200 photos for training and 100 photos for testing, for each country.

B IMPLEMENTATION DETAILS

B.1 Algorithm of MMCoA

We describe our multimodal contrastive adversarial training method, MMCoA, as presented in Algorithm 1. The relevant equations are detailed in the main text of our document.

B.2 Training Details

All the methods mentioned—CLIP (zero-shot CLIP), FT-standard, TeCoA, and our method MMCoA—employ the CLIP-B/32 architecture. This consistent choice in architecture across various techniques facilitates a direct comparison of their effectiveness and performance. The tuning of the learning rate varies between $1e-7$ and $1e-5$, and the training durations range from 10 to 30 epochs, allowing for tailored optimization according to specific method requirements and dataset characteristics. The batch size is 256.

In our comparative experiments, we adhere to the respective fine-tuning strategies for each method:

FT-standard (Full-Finetuning): We fine-tune both the image and text encoders on the clean dataset.

TeCoA: We follow its original fine-tuning approach using an SGD optimizer with a momentum of 0.9, focusing exclusively on fine-tuning the image encoder [29]. The CLIP framework includes both an image encoder and a text encoder, which facilitates the

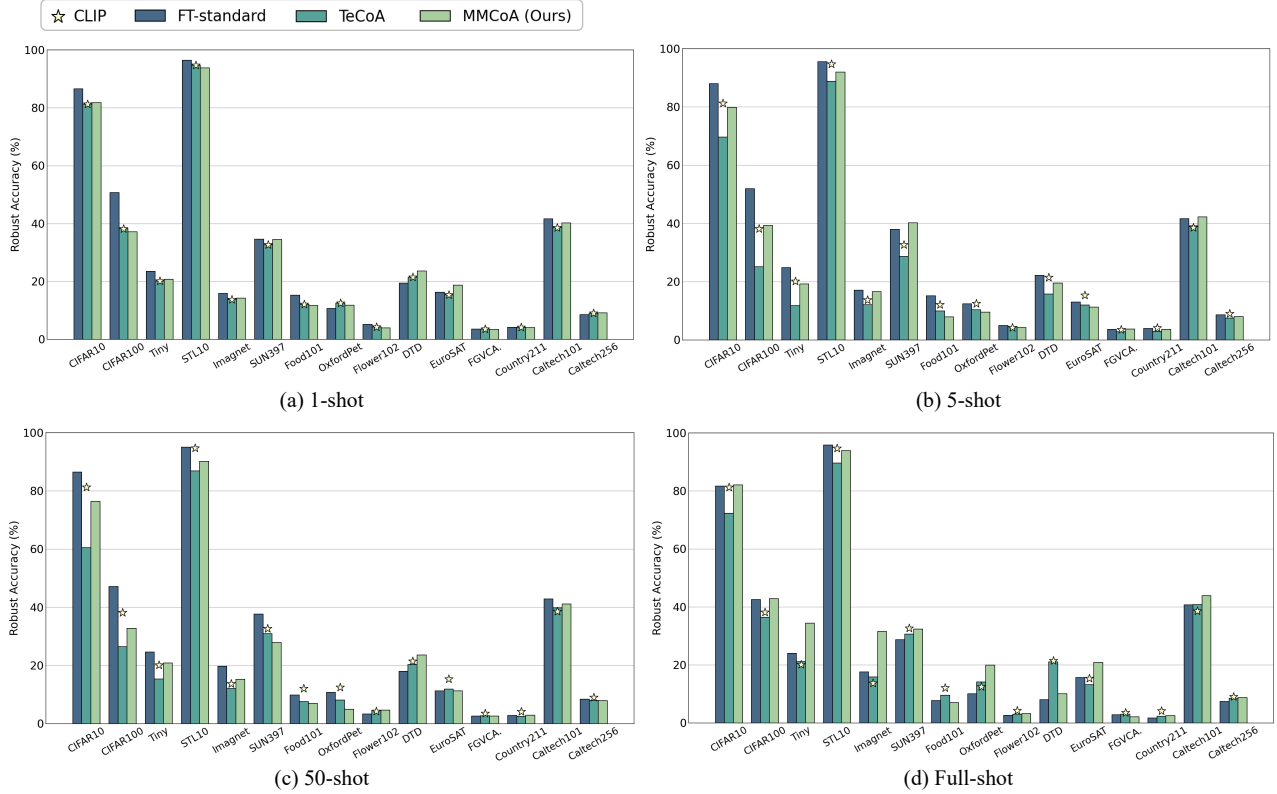


Figure 8: Out-of-distribution robust accuracies across 15 datasets under text-based BERT-Attack. We fine-tune all methods on ImageNet dataset with the few-shot setting and full-shot setting, and then test them on the remaining datasets.

Algorithm 1 MMCoA Training for Adversarial Defense in Multi-Modal Models

Require: CLIP model M , images x and class names c , perturbation bound ϵ , step size α , number of steps p , learnable parameter θ , pre-trained Bert Model B

- 1: Initialize class text prompts t for each class [CLS] in c as $t.append('This is a photo of a ' + [CLS])$
 - 2: Initialize θ with the pre-trained parameters from CLIP M
 - 3: **for** each iteration in training epochs **do**
 - 4: **for** each (x, t) in minibatch **do**
 - 5: $x_{ta} = \text{ImageAttack}(x, t, \epsilon, \alpha, p, \theta)$ {Generate adversarial image samples using the method in Eq. 1 and Eq. 2}
 - 6: $t_a = \text{BertAttack}(t, B, \theta)$ {Generate adversarial text samples using Eq. 3}
 - 7: Optimize θ to minimize \mathcal{L} as defined in Eq. 8
 - 8: **end for**
 - 9: **end for**
 - 10: **return** θ {Return the optimized parameters}
-

generation of adversarial examples in a couple of ways: 1) By connecting the image encoder to a fully connected (FC) layer, this setup allows for the training of adversarial samples specifically targeting

the image encoder; 2) By maximizing the Kullback-Leibler (KL) divergence between the image features output by the image encoder. Alternatively, the TeCoA method utilizes the full capabilities of the CLIP model by maximizing the cosine similarity between the text features and the image features, effectively creating adversarial samples. This approach is not only natural and effective but also underpins our strategy for image-based attacks. Additionally, TeCoA is an adversarial training method but only considers image-based attacks and studies the out-of-distribution zero-shot robustness of images.

MMCoA: We fine-tune the image and text encoders with multi-modal contrastive adversarial training using Algorithm 1.

C SUPPLEMENTARY EXPERIMENTS

C.1 Additional Comparisons with Baselines

C.1.1 Out-of-distribution Generalization Adversarial Robustness under Text Attack. As shown in Figure 8, we evaluate the out-of-distribution adversarial robustness across 15 datasets under text attack. When occurring with a large distribution shift, The main findings are as follows:

(1) **FT-standard achieves state-of-the-art text adversarial robustness in the few-shot setting, but its accuracy decreases and its defensive capability against text attack diminishes as the number of samples increases.** This indicates that clean

Table 4: Out-of-distribution clean accuracies across 15 datasets. Except for CLIP, we fine-tune all methods on ImageNet dataset with the few-shot setting (1-shot, 5-shot, and 50-shot) and full-shot setting, and then test them on the remaining datasets. Bold denotes the best average accuracies.

| Method | Source | | | | | Target | | | | | | | | | | Average |
|------------------|---------|---------|----------|-------|-------|--------|---------|------------|-----------|-------|---------|--------|------------|------------|------------|--------------|
| | ImagNet | CIFAR10 | CIFAR100 | Tiny. | STL10 | SUN397 | Food101 | OxfordPets | Flower102 | DTD | EuroSAT | FGVCA. | Country211 | Caltech101 | Caltech256 | |
| CLIP [33] | 59.13 | 88.57 | 62.22 | 57.90 | 97.15 | 57.64 | 83.84 | 87.38 | 65.70 | 40.21 | 38.49 | 19.98 | 15.22 | 84.91 | 87.38 | 63.05 |
| <i>1-shot</i> | | | | | | | | | | | | | | | | |
| FT-standard [40] | 63.87 | 90.03 | 67.23 | 61.89 | 97.26 | 62.42 | 84.43 | 89.32 | 65.99 | 42.61 | 47.33 | 20.85 | 15.90 | 86.69 | 83.01 | 65.26 |
| TeCoA [29] | 59.13 | 88.60 | 62.32 | 57.91 | 97.15 | 57.64 | 83.35 | 87.38 | 65.70 | 40.21 | 38.49 | 19.98 | 15.23 | 84.91 | 82.05 | 62.67 |
| MMCoA (Ours) | 58.80 | 89.87 | 62.39 | 57.69 | 97.20 | 57.98 | 83.61 | 86.56 | 65.25 | 39.95 | 40.74 | 19.80 | 15.28 | 84.27 | 81.83 | 62.75 |
| <i>5-shot</i> | | | | | | | | | | | | | | | | |
| FT-standard [40] | 65.50 | 91.43 | 68.57 | 62.34 | 96.69 | 62.27 | 83.56 | 88.66 | 63.56 | 39.04 | 45.29 | 19.14 | 16.03 | 85.64 | 82.35 | 64.67 |
| TeCoA [29] | 51.92 | 84.05 | 46.54 | 39.45 | 94.44 | 54.53 | 72.53 | 78.74 | 57.52 | 32.50 | 22.91 | 16.65 | 9.85 | 82.47 | 78.49 | 54.84 |
| MMCoA (Ours) | 57.37 | 87.00 | 55.97 | 48.96 | 94.18 | 61.28 | 72.15 | 82.97 | 57.16 | 34.47 | 30.58 | 15.00 | 12.88 | 84.58 | 79.81 | 58.29 |
| <i>50-shot</i> | | | | | | | | | | | | | | | | |
| FT-standard [40] | 61.05 | 88.87 | 61.90 | 57.46 | 96.06 | 58.18 | 75.46 | 83.51 | 54.32 | 37.71 | 22.01 | 11.37 | 13.12 | 84.04 | 80.30 | 59.02 |
| TeCoA [29] | 49.89 | 74.64 | 41.69 | 46.41 | 91.67 | 56.11 | 55.66 | 75.47 | 49.55 | 31.91 | 19.60 | 14.64 | 9.16 | 82.60 | 76.08 | 51.67 |
| MMCoA (Ours) | 60.07 | 78.63 | 48.12 | 58.67 | 90.80 | 55.93 | 60.21 | 76.81 | 46.28 | 32.39 | 23.51 | 7.53 | 9.77 | 81.02 | 76.59 | 53.76 |
| <i>Full-shot</i> | | | | | | | | | | | | | | | | |
| FT-standard [40] | 64.57 | 82.63 | 56.30 | 58.90 | 96.00 | 55.00 | 60.85 | 77.49 | 38.17 | 30.59 | 17.95 | 5.61 | 9.29 | 81.47 | 77.89 | 54.18 |
| TeCoA [29] | 63.29 | 78.31 | 49.75 | 49.79 | 93.50 | 52.72 | 55.70 | 81.77 | 51.15 | 34.10 | 26.39 | 13.86 | 8.13 | 80.26 | 76.44 | 54.34 |
| MMCoA (Ours) | 66.59 | 82.05 | 51.35 | 60.27 | 94.05 | 54.56 | 58.37 | 80.87 | 46.90 | 33.35 | 17.87 | 7.83 | 8.82 | 78.81 | 77.65 | 54.62 |

Table 5: Ablation on each constraint loss across 4 datasets with the in-distribution adversarial task. Average accuracies under three types of attacks are reported. Bold denotes the best accuracy.

| $\mathcal{L}(I' - T)$ | $\mathcal{L}(I - T')$ | Multimodal Attack | | | | Image Attack | | | |
|-----------------------|-----------------------|-------------------|--------------|--------------|--------------|--------------|--------------|--------------|--------------|
| | | CIFAR10 | CIFAR100 | Tiny. | Imagnet | CIFAR10 | CIFAR100 | Tiny. | ImagNet |
| ✓ | ✓ | 11.65 | 2.42 | 2.18 | 1.80 | 9.32 | 4.59 | 1.93 | 0.79 |
| | | 69.98 | 33.94 | 8.72 | 9.93 | 76.69 | 47.28 | 22.11 | 32.64 |
| | | 28.49 | 10.62 | 1.72 | 8.01 | 28.85 | 9.90 | 0.92 | 3.14 |
| ✓ | ✓ | 84.52 | 55.13 | 39.19 | 30.02 | 84.55 | 59.50 | 53.97 | 46.58 |
| $\mathcal{L}(I' - T)$ | $\mathcal{L}(I - T')$ | Text Attack | | | | Clean | | | |
| | | CIFAR10 | CIFAR100 | Tiny. | ImagNet | CIFAR10 | CIFAR100 | Tiny. | ImagNet |
| ✓ | ✓ | 79.74 | 37.24 | 19.67 | 13.65 | 88.56 | 62.28 | 59.46 | 59.16 |
| | | 86.75 | 47.96 | 16.34 | 13.42 | 93.42 | 70.23 | 49.98 | 53.47 |
| | | 96.74 | 83.03 | 63.14 | 50.75 | 96.70 | 83.74 | 72.31 | 51.54 |
| ✓ | ✓ | 96.16 | 75.38 | 54.13 | 41.34 | 96.17 | 81.51 | 76.11 | 67.79 |

text is more effective in defending against text attack, and it can be achieved with only a small number of image-text pairs. However, in the full-shot scenario, overfitting to the source dataset may occur, potentially leading to a decrease in adversarial robustness.

(2) **While aligning adversarial images with corresponding text, TeCoA proves ineffective under text attack.** Across all settings, TeCoA fails to surpass CLIP’s average robust accuracy.

When facing minimal distribution shifts, this training paradigm can enhance the adversarial robustness under text attack. However, this enhancement does not manifest in scenarios involving large distribution shifts.

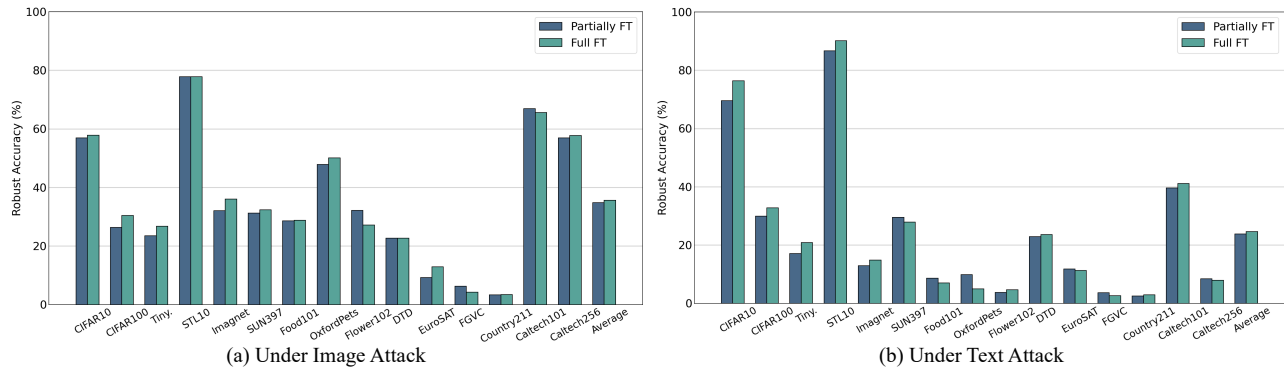


Figure 9: Exploration of the effect of the number of fine-tuned parameters with out-of-distribution generalization adversarial task on 15 datasets.

Table 6: In-distribution clean accuracies on 4 datasets. Bold denotes the best accuracies

| Method | CIFAR10 | CIFAR100 | Tiny. | ImageNet |
|------------------|--------------|--------------|--------------|--------------|
| CLIP [33] | 88.56 | 62.28 | 59.46 | 59.16 |
| FT-standard [40] | 97.01 | 85.21 | 78.96 | 64.57 |
| TeCoA [29] | 95.88 | 80.01 | 66.25 | 63.29 |
| MMCoA (Ours) | 96.17 | 81.51 | 76.11 | 67.79 |

(3) **MMCoA achieves state-of-the-art adversarial robustness in the full-shot scenario.** It indicates that multimodal adversarial training requires a substantial number of samples to effectively counter text attack.

C.2 Additional Analyses.

C.2.1 Clean Accuracy on Two Tasks. Previous work has primarily focused on studying the trade-off between robust accuracy and clean accuracy [41] of the performance of adversarial training. However, in our study, we find that: (1) *when facing minimal distribution shifts, robust accuracy and clean accuracy can be positively correlated;* (2) *when facing large distribution shifts, the trade-off between robust accuracy under multimodal and image attacks and clean accuracy continues to hold. However, there is a positive correlation trend between robust accuracy under text attack and clean accuracy.*

In-distribution Adversarial Robustness. As shown in Table 1 and Table 6, regardless of whether clean or adversarial samples are incorporated into training, we observe that all methods can outperform CLIP in terms of both robust accuracy and clean accuracy. Notably, we do not observe the phenomenon where an increase in robust accuracy leads to a decline in clean accuracy.

Meanwhile, it is intuitive to see that training with clean samples allows FT-standard to achieve state-of-the-art performance on CIFAR10, CIFAR100, and TinyImageNet. However, on ImageNet, MMCoA reaches state-of-the-art in terms of clean accuracy. This demonstrates that under minimal distribution shifts, adversarial training has the potential to simultaneously enhance both robust accuracy and clean accuracy, showcasing exceptional performance.

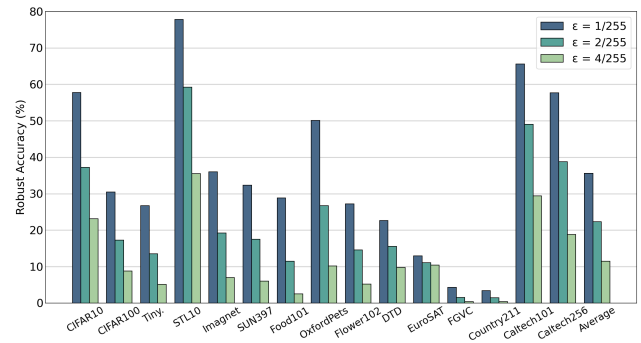


Figure 10: Exploration of the effect of the image attack strength under different perturbation bounds with out-of-distribution generalization adversarial task on 15 datasets.

Out-of-distribution Generalization Adversarial Robustness.

As illustrated in Table 4, Table 2, and Figure 3, in the few-shot setting, all methods demonstrate a trend where an increase in robust accuracy under multimodal and image attacks corresponds with a decrease in clean accuracy, indicating a clear trade-off. This observation aligns with the conclusions presented in Figure 6. In the full-shot setting, adversarial training methods exhibit some improvements in clean accuracy. Intriguingly, under text attack, the changes in text adversarial robustness closely parallel the changes in clean accuracy. Furthermore, FT-standard only surpasses CLIP in terms of average clean accuracy in the 1-shot and 5-shot settings. This enhanced performance with small sample sizes is also similar to FT-standard’s behavior under text attack.

C.2.2 Details Ablation on Each Loss. As presented in Table 5, we provide a detailed ablation study of each loss for Table 3. With the integration of two losses, MMCoA achieves state-of-the-art performance on each dataset under multimodal and image attacks. However, under text attack, it performs worse than scenarios involving only image-supervised text adversarial loss. This suggests that aligning adversarial images with clean text undermines the defense against text attack. Compared to cases with only text-supervised

adversarial loss, aligning clean images with adversarial text further enhances the defense against multimodal and image attacks.

For clean accuracy, it is evident that the image-supervised text adversarial loss contributes significantly more, particularly in datasets with fewer categories, such as CIFAR10 and CIFAR100. When dealing with datasets that have a larger number of categories, the interaction between the two losses proves to be more effective than the image-supervised text adversarial loss alone.

C.2.3 Effect of Number of Fine-tuned Parameters. As illustrated in Figure 9, we supplement the findings presented in Figure 4 of the main text by extending the comparative experiments to include scenarios under image and text attack. Consistent with our previous conclusions, full fine-tuning of the model demonstrates stronger adversarial robustness compared to partial fine-tuning.

C.2.4 Effect of Attack Strength. As depicted in Figure 10, we supplement our analysis with the impact of adversarial perturbation bounds on our method under image attack. Consistent with our previous findings, our method shows a gradual decline in robust accuracy as the adversarial perturbation increases, with the decrease exhibiting a stepwise pattern.

C.2.5 Effect of the Number of Iterations. As shown in Figure 11~14, we evaluate CLIP, TeCoA, and our method with regard to the number of training iterations for robust accuracy and clean accuracy. In the 50-shot setting, TeCoA originally trains for 10 epochs, reporting values every epoch. MMCoA, being more challenging to fit, requires additional epochs. Therefore, we demonstrate results over 28 epochs, reporting values every four epochs.

We observe that both TeCoA and MMCoA exhibit a trend where robust accuracy initially increases and then stabilizes as the number of training iterations grows under multimodal and image attacks. The performance curves for these two scenarios are quite similar.

In the case of text attack and testing on clean datasets, only a few datasets show an upward trend. Notably, apart from ImageNet, which serves as the source dataset, Caltech101 and TinyImageNet also show improvements, likely due to their relatively minor distribution differences from ImageNet. The performance curves in these cases are also similar.

D COMPREHENSIVE ANALYSES UNDER THREE TYPES OF ATTACKS ON TWO TASKS

In addition to the distribution shifts among images, we extend the concept of distribution shifts between datasets to variations in textual categories, such as differences in category types and the number of categories. Therefore, significant distribution shifts refer not only to substantial variations in image distributions but also to considerable disparities in text distributions. We provide a summary of three types of attacks across two tasks with different methods as follows.

D.1 In-distribution Adversarial Task

Adversarial Robustness. With minimal distribution shifts, by fine-tuning the CLIP model with a clean dataset, solely through image adversarial contrastive training, or through our multimodal adversarial contrastive training, all methods enhance CLIP’s adversarial robustness under three types of attacks. Adversarial training

is particularly effective under multimodal and image attacks. Additionally, our multimodal contrastive adversarial training (MMCoA) demonstrates superior adversarial robustness in more complex datasets, such as those with a greater number of categories, across all three types of attacks.

Clean Accuracy. When facing minimal distribution shifts, there is often a positive correlation between robust accuracy and clean accuracy, indicating that the traditional trade-off between robustness and performance may not hold under these conditions. Moreover, fine-tuning the CLIP model with a clean dataset yields optimal clean accuracy on CIFAR10, CIFAR100, and TinyImageNet. However, for ImageNet, the MMCoA method achieves state-of-the-art clean accuracy, underscoring the potential of adversarial learning to enhance clean accuracy when fine-tuning specific datasets with adversarial examples on large-scale multimodal models like CLIP.

D.2 Out-of-distribution Generalization Adversarial Task

Adversarial Robustness. With large distribution shifts, all three methods still enhance CLIP’s adversarial robustness under two types of attacks in both few-shot and full-shot settings, *i.e.*, multimodal and image attacks, achieving optimal performance in the full-shot scenario. Moreover, our multimodal adversarial contrastive training effectively balances efficiency, effectiveness, and robustness. However, for text attack, none of the methods significantly enhance CLIP’s robustness, indicating that defense strategies against text attack require further exploration. We hope this study can serve as a foundation for future research to develop more effective methods for combating text-based adversarial threats.

Clean Accuracy. When facing large distribution shifts, there is a clear trade-off between robust accuracy under multimodal and image attacks and clean accuracy, consistent with previous research that adversarial training can compromise performance on clean datasets. Interestingly, the variations in robust accuracy under text attack show a certain similarity to changes in clean accuracy.

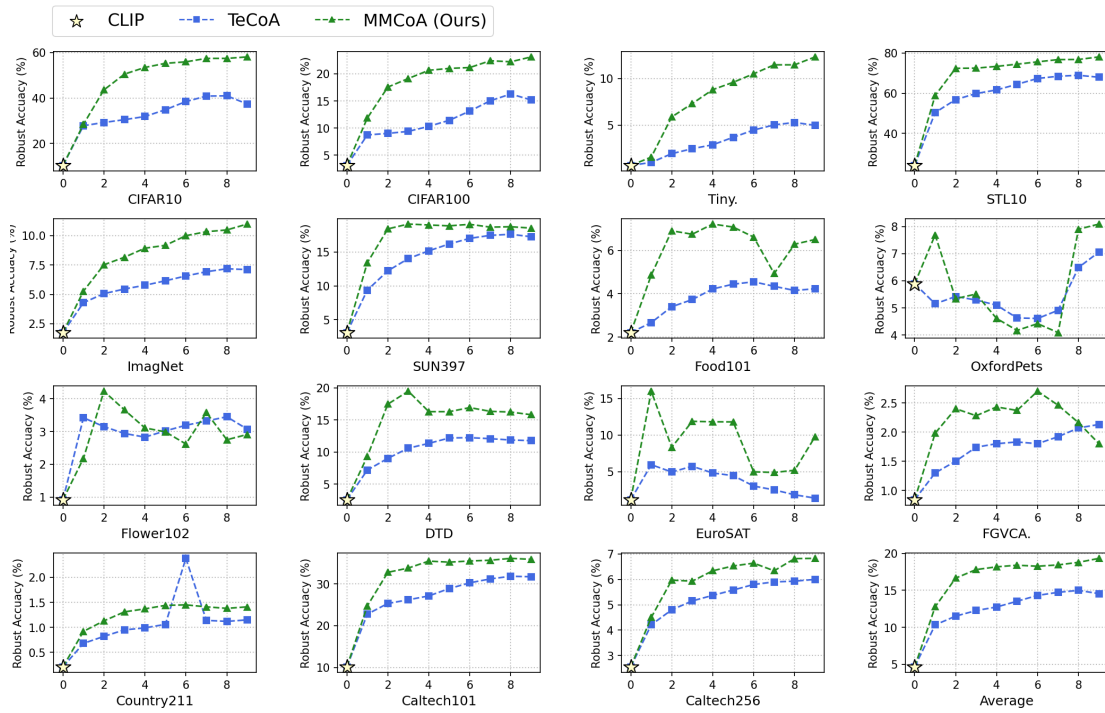


Figure 11: Effect of the number of iterations on 50-shot out-of-distribution generalization adversarial task for CLIP, TeCoA, and our MMCoA across 15 datasets under multimodal attack.

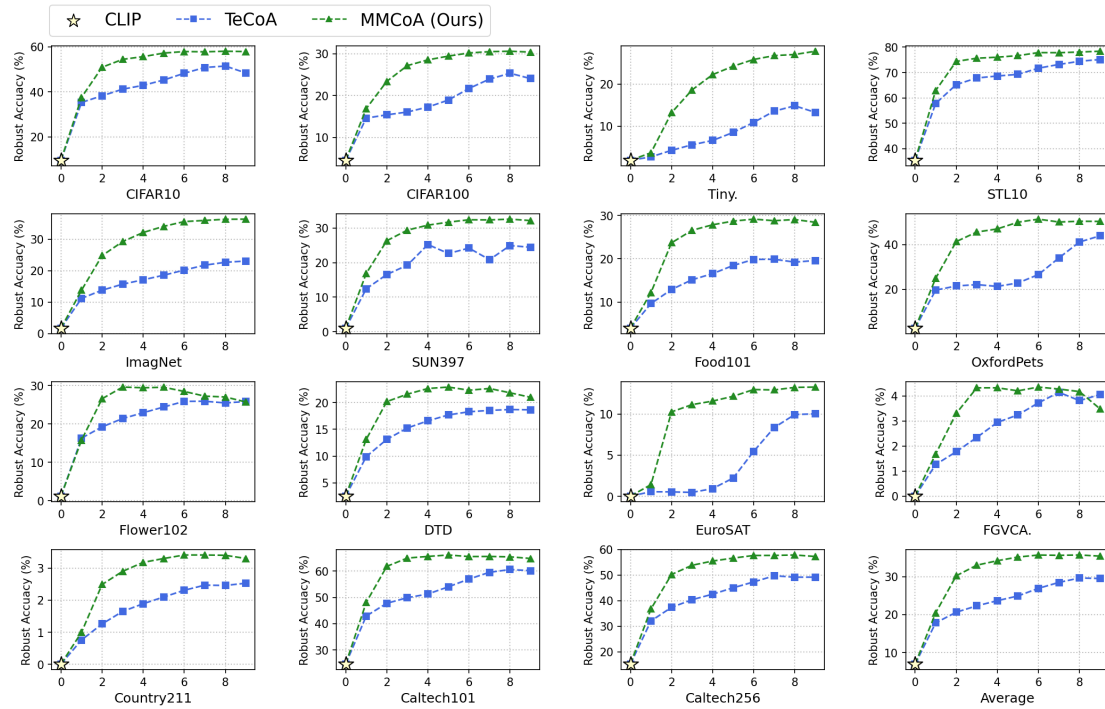


Figure 12: Effect of the number of iterations on 50-shot out-of-distribution generalization adversarial task for CLIP, TeCoA, and our MMCoA across 15 datasets under image attack.

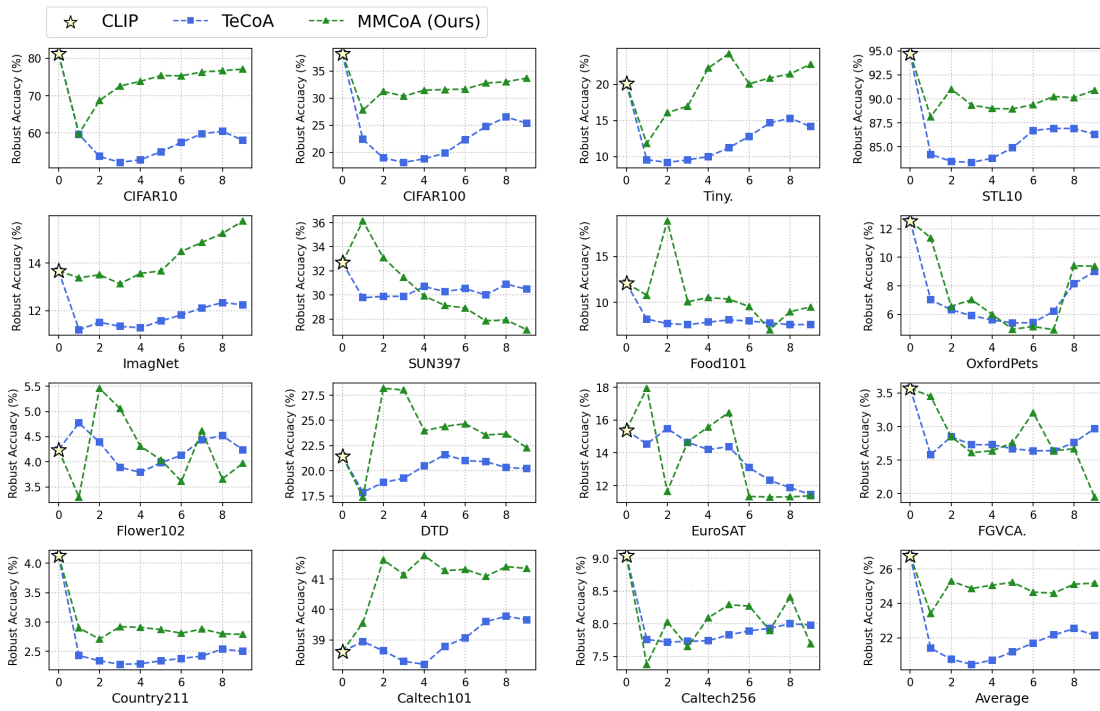


Figure 13: Effect of the number of iterations on 50-shot out-of-distribution generalization adversarial task for CLIP, TeCoA, and our MMCoA across 15 datasets under text attack.

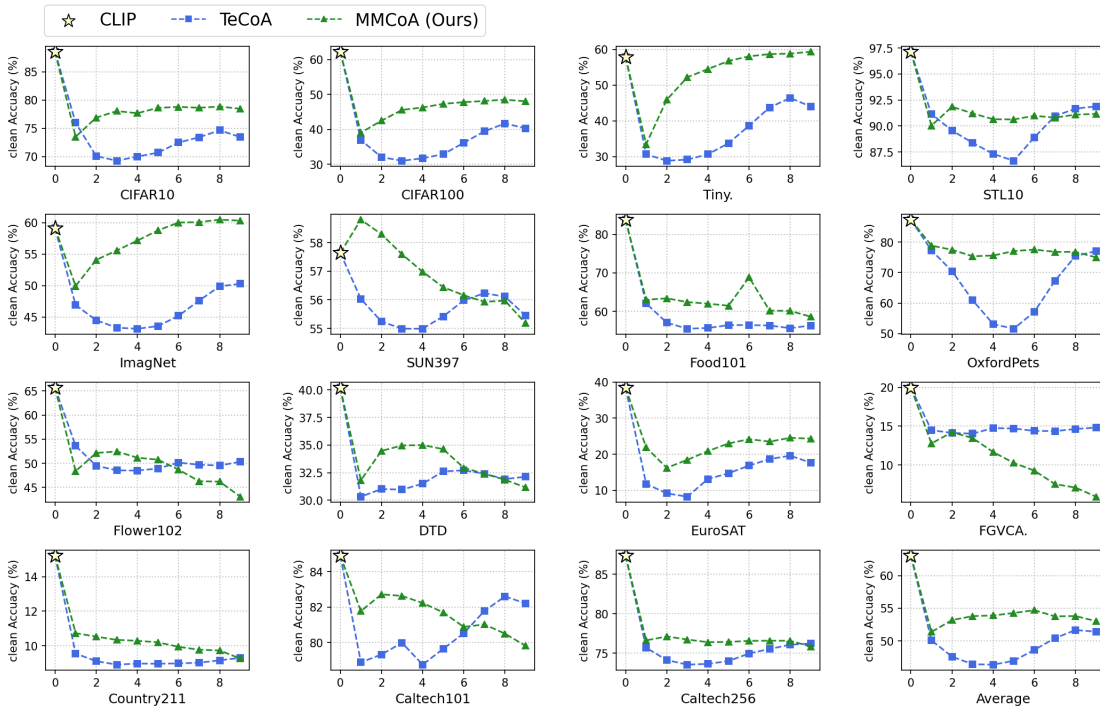


Figure 14: Effect of the number of iterations on 50-shot out-of-distribution generalization adversarial task for CLIP, TeCoA, and our MMCoA across 15 datasets with clean accuracy.